Identification of the Silicon Vacancy Containing a Single Hydrogen Atom by EPR

B. Bech Nielsen, P. Johannesen, P. Stallinga, and K. Bonde Nielsen
Institute of Physics and Astronomy, University of Aarhus, DK-8000 Århus C, Denmark

J. R. Byberg
Institute of Chemistry, University of Aarhus, DK-8000 Århus C, Denmark
(Received 17 March 1997)

The electron paramagnetic resonance spectrum of float-zone silicon recorded after implantation with protons contains a strongly temperature dependent signal from a vacancy-type defect. The signal displays monoclinic-I symmetry below 65 K and trigonal symmetry above 100 K. This symmetry change, together with a hyperfine splitting from a single proton, allows an unequivocal identification with VH^0, the neutral charge state of a vacancy containing a single hydrogen atom. The striking similarity between the properties of VH^0 and VP^0 (the E center) corroborate our identification. [S0031-9007(97)03778-2]

PACS numbers: 61.72.Tt, 71.55.Ak, 76.30.Mi

The electrical and optical properties of hydrogen in crystalline silicon have been intensively studied during the past decade [1]. Detailed information on the structure of hydrogen-related defects is an essential prerequisite for understanding such properties. Thus, the technological applications of hydrogen as a modifier of the electrical properties of the material benefit from a continued search for the structures of hydrogen-related defects. Moreover, the ultimate electronic simplicity of hydrogen makes such structures an excellent testing ground for *ab initio* calculations. In spite of this, few defect structures involving hydrogen have been rigorously established [2–5]. In the present work, we identify a fundamental hydrogen-related defect, the existence of which has been suspected for more than a decade.

In molecular compounds, hydrogen and silicon form strong, covalent Si-H bonds with a dissociation energy of about 3.3 eV [6]. Hence, any defect that allows formation of such bonds will constitute a deep trap for hydrogen. The monovacancy is such a structure. Each of its four silicon neighbors are tricoordinated, which leaves one of their four valence orbitals free to form a bonding combination with a hydrogen 1s orbital. Direct evidence for this was recently obtained by analysis of the infrared absorption spectrum of proton-implanted silicon, in which the Si-H stretch modes belonging to the monovacancy binding two, three, and four hydrogen atoms were identified [4]. Thus, vacancy-hydrogen defects are known to exist, but their electronic properties remain to be established experimentally. Moreover, the simplest defect of this type, the monovacancy containing a single hydrogen atom VH, has yet to be identified.

The electronic properties expected for VH^0 (the neutral charge state of VH) may be outlined as follows: The one-electron energy of the bonding combination of the hydrogen 1s orbital and the silicon orbital will be located well below the top of the valence band, because the ionization potential of hydrogen (13.6 eV) greatly exceeds the minimum energy required to lift an electron from the valence band to the lowest vacuum state. The energy of the corresponding antibonding combination is expected to lie well above the edge of the conduction band, owing to the strong overlap of the two orbitals. Therefore, any electronic level of VH^0 that lies within the band gap must correspond to a combination of the remaining three silicon orbitals. Two of these may combine to form a long Si-Si bond perpendicular to a {100} mirror plane, while that lying in the mirror plane is occupied by a single electron and is commonly referred to as a dangling bond. Thus, VH^0 should have monoclinic-I symmetry (point group C_{1h}) with the Si-H bond bent a few degrees away from a $\langle 111 \rangle$ axis in the mirror plane. These expectations are supported by the results of *ab initio* calculations [7,8].

The structure outlined for VH^0 corresponds closely to that of the E center (VP^0), in which a substitutional phosphorous atom is located next to a monovacancy [9]. Hence, we may expect the electron spin distribution of VH^0 to resemble that deduced from the electron paramagnetic resonance (EPR) signal of VP^0. VH^0 might also have other properties in common with VP^0, such as the dramatic temperature dependence of the EPR signal: Above 90 K, VP^0 exhibits an effective trigonal symmetry due to thermally activated jumps of the dangling bond among the three silicon atoms neighboring the vacancy.

This Letter reports the identification of VH^0 by EPR in proton-implanted silicon. The observed properties, including a thermally activated transition from monoclinic-I symmetry to an effective trigonal symmetry, all testify to the expected similarity with VP^0.

Samples measuring $\sim 4 \times 3 \times 1$ mm^3, with the large faces normal to the [111] axis, were cut from uncompensated n-type float-zone silicon. The quoted resistivity was 600 Ω cm corresponding to a phosphorus concentration of

$\sim 9 \times 10^{12}$ cm^{-3}. The concentration of other impurities, mainly carbon and oxygen, were below 3×10^{16} cm^{-3}. The samples were polished on both large faces and then etched lightly to remove surface defects that might give rise to EPR signals. The samples were implanted at low temperature ($T \lesssim 150$ K) with protons (or deuterons) on both large faces at 56 (or 38) different energies in the range from 5.3 to 10.5 MeV (or 5.0 to 10.6 MeV) [10]. During implantation with protons, the sample was covered with 0.2 mm aluminum. The dose implanted at each energy was adjusted to ensure a uniform hydrogen concentration of $\sim 3 \times 10^{17}$ cm^{-3} throughout the sample. At this dose level, the line shape of the resulting EPR signal was unaffected by the radiation damage produced by the implantation. Subsequent to the implantation, the samples were allowed to warm up to room temperature.

EPR measurements were made at 9.2 and 35 GHz in the absorption mode with a Bruker ESP300E spectrometer. The static magnetic field $\mathbf{B}_0$ was monitored continuously during the scans with a Bruker ER-035 NMR gaussmeter. Resolution enhancement by third harmonic detection [11,12] was employed in most of the measurements. Thus, the magnetic field was modulated at 33 and 100 kHz simultaneously, and the EPR signal was detected at 100 kHz. By a judicious choice of the modulation amplitudes, the effective EPR linewidth could be reduced without the appearance of spurious lines.

EPR spectra were recorded with $\mathbf{B}_0$ lying in the $(1\bar{1}0)$ plane of the sample at 5° intervals. Because the proton hyperfine coupling of the defect discussed here is much smaller than the nuclear Zeeman energy of the proton at the employed magnetic field, the hyperfine splitting observed *between* the principal directions strongly reflects the relative signs of the principal values of the hyperfine tensor. These signs could therefore be determined unambiguously from computer simulations of certain EPR spectra with different choices of the signs.

Owing to the absence of resolved hyperfine splittings from the implanted deuterons, the EPR spectra obtained from the deuteron-implanted sample Si:D are somewhat simpler to analyze than those from Si:H. Therefore, we first discuss the EPR signal from Si:D. Anticipating the identification made below, we label the corresponding defect by VH^0, irrespective of the actual hydrogen isotope. In Fig. 1, we show the EPR spectra of Si:D recorded at temperatures in the range 45–225 K with $\mathbf{B}_0$ parallel to [111]. The intense, narrow lines observed at 225 K are attributed to two components of the S1 signal [5,13] which have been observed previously in proton-implanted silicon. These lines are observable throughout the temperature range, but they become partially saturated below 85 K at the applied microwave power. At 45 K, the spectrum exhibits three additional lines *A*, *B*, and *C*, which we assign to VH^0. The line *A* almost coincides with one of the lines of the S1 signal. As the temperature is raised, the widths of the lines *A* and *B* increase and at 85 K these lines disappear, whereas line *C* persists. Above 110 K, a new line *AB* emerges at a position one-third the distance from *A* to *B*. The line *AB* attains maximum height (minimum linewidth) at 145 K. At higher temperatures, the lines

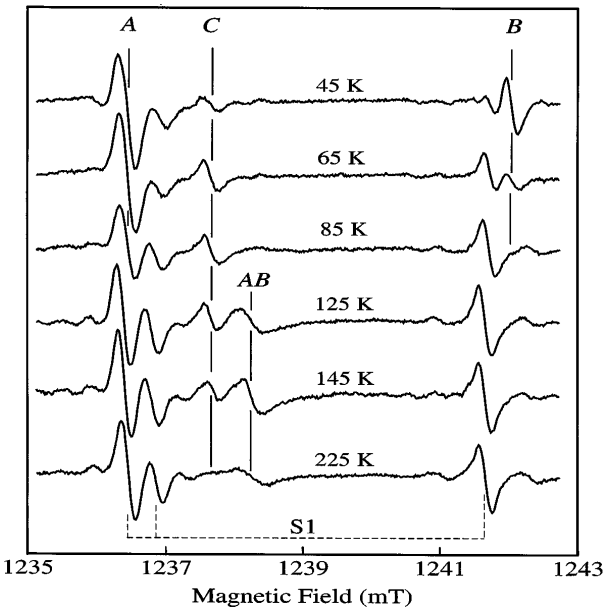

FIG. 1. EPR spectra recorded at different sample temperatures at 34.778 GHz with $\mathbf{B}_0$ along the [111] axis. The lines denoted *A*, *B*, *C*, and *AB* originate from VH^0.

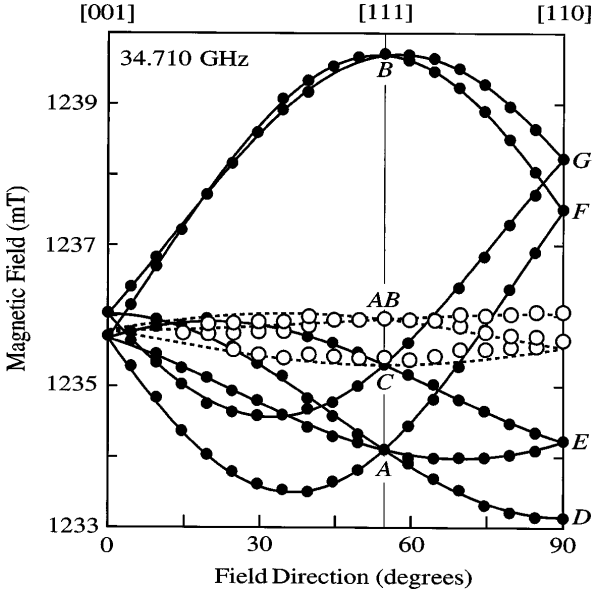

FIG. 2. Angular variation in the $(1\bar{1}0)$ plane of the positions of the EPR lines of VH^0. (•) Represents measurements at 45 K and (○) represents measurements at 145 K. Solid lines are calculated for a monoclinic-I center with $S = 1/2$ and the *g* tensor given in Table I. Dashed lines represent a trigonal signal corresponding to the algebraic mean of the *g* tensors for one set of configurations (see text). *A*, *B*, *C*, *D*, *E*, *F*, *G*, and *AB* denote the positions of the lines shown in Figs. 1 and 3.

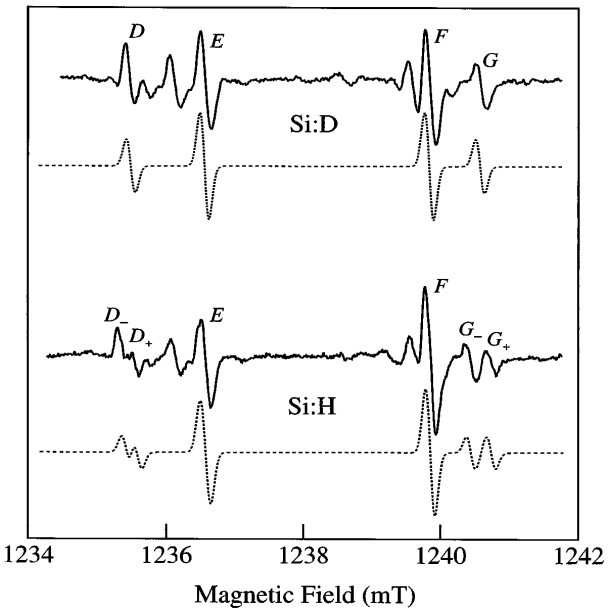

FIG. 3. Solid curves: EPR spectra of Si:D and Si:H recorded at 45 K and at 34.777 GHz with $\mathbf{B}_0$ along [110]. The lines denoted D, $D_{\pm}$, E, F, G, and $G_{\pm}$ originate from VH^0. The additional lines belong to other vacancy-type defects. Dashed curves: simulations of the VH^0 signal at 45 K based on the parameters in Table I.

C and AB broaden and become unobservable at room temperature.

The observation that the VH^0 signal recorded at a low temperature with $\mathbf{B}_0 \parallel [111]$ consists of three lines suggests that the defect has monoclinic-I symmetry. This is confirmed by the angular variation of the signal in the $(1\bar{1}0)$ plane measured at 45 K, which is shown in Fig. 2. The 12 equivalent configurations of a monoclinic-I defect can be subdivided into four sets, each associated with a particular $\langle 111 \rangle$ axis, so that the members of a given set are interrelated through 120° (C_3) rotations about the pertinent $\langle 111 \rangle$ axis. The temperature dependence of the VH^0 signal can be explained as a result of thermally activated jumps among the three configurations of each set. The set defined by the [111] axis contributes solely to line C in Fig. 1 and, therefore, this line is unaffected by the jumps. In contrast, the other three sets all contribute to both line A and line B. Consequently, a defect switching among the configurations within one of these sets contributes alternatingly to line A and line B. As the temperature is raised, the jump frequency ν_j increases and the lines A and B therefore become broadened. When the temperature becomes so high that ν_j exceeds the spectral separation of A and B in frequency units, a single line arises due to motional narrowing [14] at a position that is the weighted average of the original positions of A and B. This interpretation implies that the VH^0 signal should exhibit trigonal symmetry above 110 K. The angular dependence of the VH^0 signal expected from the jump model in this limit may be calculated from the g tensor measured at 45 K. The result is included in Fig. 2 (dashed curves) along with positions of the EPR lines observed at 145 K. The good agreement justifies the assignment of the high-temperature signal to VH^0. As described by Watkins and Corbett [9], the activation energy E_a of the jump process can be estimated from the temperature dependence of the linewidths in the regions corresponding to broadening and motional narrowing. The result is $E_a = 0.06 \pm 0.01$ eV.

The involvement of a single hydrogen atom in VH^0 is demonstrated in Fig. 3 which shows the spectra of Si:D and Si:H recorded with $\mathbf{B}_0$ along [110]. The VH^0 lines observed in Si:D are labeled by D through G. In the signal from Si:H, the lines D and G appear as doublets due to hyperfine interaction with a single proton. The absence of a resolved splitting of the lines E and F reflects that the hyperfine splitting is strongly anisotropic. We note that the hyperfine splitting for the deuteron calculated from that for the proton is smaller than the linewidth for all orientations of $\mathbf{B}_0$.

In addition to the proton hyperfine splitting, each of the main lines of the VH^0 signal in both Si:H and Si:D has a pair of weak satellite lines. The intensity of these satellites relative to the main line is $\sim 2\%$, and we ascribe them to the hyperfine interaction with a single ^{29}Si nucleus.

The spin-Hamiltonian parameters of VH^0 are presented in Table I. The g tensor of VH^0 is almost trigonal, i.e., $g_X \approx g_Y$, and the unique axis Z deviates by only 3° from the [111] axis, while the ^{29}Si hyperfine tensor is trigonal within the limits of error. The values of

TABLE I. Spin-Hamiltonian parameters for VH^0 at 45 K and for VP^0 (Ref. [9]). Principal axes are denoted X, Y, Z, with Y parallel to the $[1\bar{1}0]$ axis and X, Z spanning the $(1\bar{1}0)$ plane. Θ is the angle between Z and the [110] axis. Hyperfine parameters $\mathbf{A}$ are given in MHz. Limits of error: $\mathbf{g}$, ± 0.0001; $\mathbf{A}(^{29}\mathrm{Si})$, ± 1 MHz; $\mathbf{A}(^{1}\mathrm{H})$, ± 0.3 MHz.

Defect	Term	X	Y	Z	Θ
VH^0	$\mathbf{g}$	2.0090	2.0114	2.0006	32.4°
VH^0	$\mathbf{A}(^{1}\mathrm{H})$	−3.3	−4.6	8.5	8°
VH^0	$\mathbf{A}(^{29}\mathrm{Si})$	−275	−275	−435	35.3°
VP^0	$\mathbf{g}$	2.0096	2.0112	2.0005	32°
VP^0	$\mathbf{A}(^{29}\mathrm{Si})$	−295	−295	−450	35.3°

the spin-Hamiltonian parameters closely resemble those for VP^0, also given in the table, and are typical for centers which have the electron spin largely confined to a dangling-bond orbital in a vacancy-type defect [15]. Furthermore, the transition from a monoclinic-I signal to a trigonal signal has the same activation energy as the corresponding transition of the VP^0 signal, indicating that the underlying processes are identical. These observations justify the identification of the defect with the neutral charge state of the monovacancy containing a single hydrogen atom, as implied by the label VH^0.

Additional support for this identification comes from an analysis of the proton hyperfine splitting. The absence of a significant isotropic component (Table I) indicates a vanishing electron spin density at the proton. Therefore, the observed anisotropic splitting represents a dipolar coupling of the proton spin to the electron spin residing primarily in the dangling-bond orbital centered on a "distant" silicon atom. The unique axis Z of $\mathbf{A}(^1\mathrm{H})$ deviates by only 8° from the [110] axis, in accordance with our assignment which implies that the vector $\boldsymbol{R}$ from the proton to the silicon atom carrying the dangling bond points roughly in a [110] direction. The dipolar hyperfine parameter $b \equiv \frac{1}{6}(2A_Z - A_X - A_Y)$ has the value $b = 4.1$ MHz. Within the point-dipole approximation, the distance $\|\boldsymbol{R}\|$ may be estimated from the expression $b = g_e \mu_B g_N \mu_N \|\boldsymbol{R}\|^{-3}$, where g_e and g_N are the g values of the electron and proton, and μ_B and μ_N are the Bohr and nuclear magneton. The result is $\|\boldsymbol{R}\| = 2.7$ Å, in good agreement with the value 2.8 Å calculated from the unrelaxed geometry of VH^0, with the 1.5 Å Si-H bond along a ⟨111⟩ axis. Moreover, the structure of the H1 defect [16] in diamond is believed to resemble that of VH^0. Hence, it is interesting to note that our value of $\|\boldsymbol{R}\|$ and the hydrogen-dangling-bond distance of the H1 defect scale with the ratio of the lattice constants of silicon and diamond.

We conclude that VH^0 is present in proton-implanted silicon and that its electronic properties are determined almost completely by the silicon dangling bond. The similarity of the spin Hamiltonians of VH^0 and VP^0 (E center) indicates that the Si-H fragment in this context may be regarded as a "pseudo-group-V impurity."

This work was supported by the Danish National Research Foundation through the Aarhus Center for Advanced Physics (ACAP).

[1] See, e.g., S. J. Pearton, J. W. Corbett, and M. Stavola, *Hydrogen in Crystalline Semiconductors* (Springer-Verlag, Berlin, 1992); *Hydrogen in Semiconductors*, Semiconductors and Semimetals Vol. 34, edited by J. I. Pancove and N. M. Johnson (Academic Press, Boston, 1991).
[2] K. Bergman, M. Stavola, S. J. Pearton, and T. Hayes, Phys. Rev. B **38**, 9643 (1988).
[3] J. D. Holbech, B. Bech Nielsen, R. Jones, P. Sitch, and S. Öberg, Phys. Rev. Lett. **71**, 875 (1993).
[4] B. Bech Nielsen, L. Hoffmann, and M. Budde, Mater. Sci. Eng. B **36**, 259 (1996).
[5] Yu. V. Gorelkinskii and N. N. Nevinnyi, Physica (Amsterdam) **170B**, 155 (1991).
[6] T. L. Cottrell, *The Strength of Chemical Bonds* (Butterworths, London, 1954), p. 273.
[7] P. Deák, L. C. Snyder, M. Heinrich, C. R. Ortiz, and J. W. Corbett, Physica (Amsterdam) **170B**, 253 (1991).
[8] M. A. Roberson and S. K. Estreicher, Phys. Rev. B **49**, 17 040 (1994).
[9] G. D. Watkins and J. W. Corbett, Phys. Rev. **134**, A1359 (1964).
[10] Although these implantation energies exceed the Coulomb barrier (~3 MeV) for nuclear reaction between ^{1}H and ^{28}Si, the small cross section makes the production of impurities (e.g., phosphorus) insignificant.
[11] L. C. Allen, J. Chem. Phys. **40**, 3135 (1964).
[12] S. H. Glarum, Rev. Sci. Instrum. **36**, 771 (1965).
[13] H. Lütgemeier and K. Schnitzke, Phys. Lett. **25A**, 232 (1967).
[14] H. S. Gutowsky and A. Saika, J. Chem. Phys. **21**, 1688 (1953).
[15] Y. H. Lee and J. W. Corbett, Phys. Rev. B **8**, 2810 (1973).
[16] X. Zhou, G. D. Watkins, K. M. McNamara Rutledge, R. P. Messmer, and S. Chawla, Phys. Rev. B **54**, 7881 (1996).